Inorg. Chem. **2008**, *47*, 4368−4374

Syntheses, Crystal Structures, and Physical Properties of $La_5Cu_6O_4S_7$ and $La_5Cu_{6.33}O_4S_7$

George H. Chan,[†] Ming-Ling Liu,[‡,§] Li-Dong Chen,[§] Fu-Qiang Huang,[*,§] Daniel E. Bugaris,[†] Daniel M. Wells,[†] John R. Ireland,[⊥] Mark C. Hersam,[†,⊥] Richard P. Van Duyne,[†] and James A. Ibers[*,†]

Department of Chemistry, Northwestern University, 2145 Sheridan Road, Evanston, Illinois 60208-3113, Graduate School of the Chinese Academy of Science, Beijing, 1000039, P.R. China, Shanghai Institute of Ceramics, Chinese Academy of Science, 1295 Ding-Xi Road, Shanghai, 200050, P.R. China, and Department of Materials Science and Engineering, Northwestern University, 2220 Campus Drive, Cook Hall, Evanston, Illinois, 60208-3108

Received December 21, 2007

Single crystal and bulk powder samples of the quaternary lanthanum copper oxysulfides $La_5Cu_{6.33}O_4S_7$ and $La_5Cu_6O_4S_7$ have been prepared by means of high-temperature sealed-tube reactions and spark plasma sintering, respectively. In the structure of $La_5Cu_{6.33}O_4S_7$, Cu atoms tie together the fluorite-like $^2_\infty[La_5O_4S^{5+}]$ and antifluorite-like $^2_\infty[Cu_6S_6^{5-}]$ layers of $La_5Cu_6O_4S_7$. The optical band gap, E_g, of 2.0 eV was deduced from both diffuse reflectance spectra on a bulk sample of $La_5Cu_6O_4S_7$ and for the (010) crystal face of a $La_5Cu_{6.33}O_4S_7$ single crystal. Transport measurements at 298 K on a bulk sample of $La_5Cu_6O_4S_7$ indicated *p*-type metallic electrical conduction with $\sigma_{electrical} = 2.18$ S cm^{-1}, whereas measurements on a $La_5Cu_{6.33}O_4S_7$ single crystal led to $\sigma_{electrical} = 4.5\ 10^{-3}$ S cm^{-1} along [100] and to semiconducting behavior. In going from $La_5Cu_6O_4S_7$ to $La_5Cu_{6.33}O_4S_7$, the disruption of the $^2_\infty[Cu_6S_6^{5-}]$ layer and the decrease in the overall Cu^{2+} ($3d^9$) concentration lead to a significant decrease in the electrical conductivity.

Introduction

Materials that exhibit optical transparency in the visible region and *p*-type electrical conductivity comparable to those of ZnO- and InSnO-based *n*-type transparent conductors are scarce. The best known transparent *p*-type materials have conductivities 10−100 times smaller than those of typical *n*-type conductors. These include *p*-type $CuAlO_2$ thin films, which can have conductivities as large as 1 S cm^{-1},[1,2] and $CuMO_2$ (M = Ga, In, Sc, Y) delafossites[3–5] and Cu_2SrO_2[6–8] with conductivities in the range 0.004−40 S cm^{-1}.

The compounds LnCuOQ (Ln = rare-earth metal; Q = chalcogen) are wide band gap *p*-type materials with fluorite-like $^2_\infty[Ln_2O_2^{2+}]$ and antifluorite-like $^2_\infty[Cu_2Q_2^{2-}]$ layers stacked perpendicular to the *c*-axis of a tetragonal cell.[9–11] The formal oxidation state of Cu is +1 in these compounds and the $^2_\infty[Cu_2Q_2^{2-}]$ layer is the origin for *p*-type electrical conduction.[11] Chemical manipulation of the $^2_\infty[Ln_2O_2^{2+}]$ or $^2_\infty[Cu_2Q_2^{2-}]$ layers leads to new materials with interesting physical properties, as demonstrated in the com-

* To whom correspondence should be addressed. E-mail: huangfq@mail.sic.ac.cn (F.Q.H.), ibers@chem.northwestern.edu (J.A.I.). Fax: +86 21 52413903 (F.Q.H.), +1 847 491 2976 (J.A.I.). Phone: +1 847 491 5449(J.A.I.).

† Department of Chemistry, Northwestern University.

‡ Graduate School of the Chinese Academy of Science.

§ Shanghai Institute of Ceramics.

⊥ Department of Materials Science and Engineering, Northwestern University.

(1) Kawazoe, H.; Yasukawa, M.; Hyodo, H.; Kurita, M.; Yanagi, H.; Hosono, H. *Nature (London)* **1997**, *389*, 939–942.

(2) Yanagi, H.; Inoue, S.-ichiro; Ueda, K.; Kawazoe, H.; Hosono, H.; Hamada, N. *J. Appl. Phys.* **2000**, *88*, 4159–4163.

(3) Yanagi, H.; Hase, T.; Ibuki, S.; Ueda, K.; Hosono, H. *Appl. Phys. Lett.* **2001**, *78*, 1583–1585.

(4) Yanagi, H.; Ueda, K.; Ohta, H.; Orita, M.; Hirano, M.; Hosono, H. *Solid State Commun.* **2002**, *121*, 15–18.

(5) Ingram, B. J.; Harder, B. J.; Hrabe, N. W.; Mason, T. O.; Poeppelmeier, K. R. *Chem. Mater.* **2004**, *16*, 5623–5629.

(6) Duan, N.; Sleight, A. W.; Jayaraj, M. K.; Tate, J. *Appl. Phys. Lett.* **2000**, *77*, 1325–1326.

(7) Kudo, A.; Yanagi, H.; Hosono, H.; Kawazoe, H. *Appl. Phys. Lett.* **1998**, *73*, 220–222.

(8) Nagarajan, R.; Duan, N.; Jayaraj, M. K.; Li, J.; Vanaja, K. A.; Yokochi, A.; Draeseke, A.; Tate, J.; Sleight, A. W. *Int. J. Inorg. Mater.* **2001**, *3*, 265–270.

(9) Palazzi, M.C. R. *Acad. Sci., Sér. 2* **1981**, *292*, 789–791.

(10) Ueda, K.; Takafuji, K.; Hiramatsu, H.; Ohta, H.; Kamiya, T.; Hirano, M.; Hosono, H. *Chem. Mater.* **2003**, *15*, 3692–3695.

(11) Ueda, K.; Hiramatsu, H.; Hirano, M.; Kamiya, T.; Hosono, H. *Thin Solid Films* **2006**, *496*, 8–15.

10.1021/ic7024796 CCC: $40.75
Published on Web 04/23/2008

pounds $CeCu_{0.8}OS$,[12] $CeMn_{0.5}OSe$,[13] $La_2CdO_2Se_2$,[14] and $La_5Cu_6O_4S_7$.[15] The structure of $La_5Cu_6O_4S_7$, which formally contains one Cu^{2+} and five Cu^{1+} centers, is similar to that of LaCuOS, comprising $^2_\infty[La_5O_4S^{5+}]$ and $^2_\infty[Cu_6S_6^{5-}]$ layers stacked perpendicular to the *c*-axis of a tetragonal cell. The electrical conductivity along [100] was determined to be 2.6×10^4 S cm^{-1} at 298 K.[15] However, the available crystals were too small to allow the determination of the type and number of charge carriers present in the material. Moreover, the optical properties were not investigated.

Our attempts to resynthesize single crystals of $La_5Cu_6O_4S_7$ for transport and optical measurements have led to the synthesis of single crystals of the nonstoichiometric but closely related compound $La_5Cu_{6.33}O_4S_7$. We describe here details of that synthesis and structure, as well as the results of optical and transport measurements. We also describe the synthesis and some physical measurements on a bulk powder sample of $La_5Cu_6O_4S_7$.

Experimental Section

Syntheses of $La_5Cu_6O_4S_7$ and LaCuOS Powders. The synthesis of orange single crystals of $La_5Cu_6O_4S_7$ has been described previously.[15] Attempts to repeat this synthesis failed to produce single crystals of $La_5Cu_6O_4S_7$ despite numerous variations of the procedure. However, a powder sample could be synthesized. Both $La_5Cu_6O_4S_7$ and LaCuOS powders were synthesized by the solid-state reactions of stoichiometric amounts of La_2O_3 (99.99%, SinoReag), Cu (99.999%, SinoReag), La_2S_3 (99%, Strem), and S (99.999%, SinoReag). La_2O_3 was kept at 1223 K for 12 h and then cooled and kept under vacuum until used. The powders were sealed in fused-silica tubes and evacuated to $<5 \times 10^{-2}$ Torr under Ar. The samples were slowly heated to 1123 K in 26 h, kept at 1123 K for 72 h, and then the furnace was turned off and allowed to cool to 298 K. The harvested powders were ground and then loaded into fused-silica tubes. The tubes were evacuated and sealed, and then subjected to the same heating sequence as before. The final powders were densified in an Ar atmosphere under a pressure of 60 MPa in a graphite die (10 mm diameter) in a spark plasma sintering furnace at 1073 K for 4 min.

Powder Diffraction Measurements of $La_5Cu_6O_4S_7$ and LaCuOS Powders. X-ray powder diffraction patterns on powders of $La_5Cu_6O_4S_7$ and LaCuOS were obtained on a Rigaku D/Max-2550 V diffractometer with the use of Cu Kα radiation ($\lambda = 1.5418$ Å). The scan speed was 4°/min, the voltage was 40 kV, and the current was 40 mA.

Diffuse Reflectance of $La_5Cu_6O_4S_7$ and LaCuOS Powders. The optical absorption spectra of pulverized powders of $La_5Cu_6O_4S_7$ and LaCuOS were measured at 298 K by means of a UV−vis-NIR spectrometer (Hitachi UV-3010PC) equipped with an integrating sphere.

Transport Measurements of Sintered Discs of $La_5Cu_6O_4S_7$ and LaCuOS. Electrical conductivity measurements were made by means of the four-probe method from 150 to 450 K. The Hall effect was investigated on an Accent HL5500 Hall System at 298 K. Silver paste was used for the electrodes, and ohmic contact was confirmed before measurements were made. The Seebeck coefficient was measured by a two-probe method from 250 to 500 K; the thermocouple was made of Pt and Pt/Rh.

Synthesis of Single Crystals of $La_5Cu_{6.33}O_4S_7$. The following reagents were first checked for purity by powder X-ray diffraction methods, then ground with a mortar and pestle, and loaded into a fused-silica tube under ambient conditions. Red-colored single crystals of $La_5Cu_{6.33}O_4S_7$ were synthesized by the solid-state reaction of stoichiometric amounts of La_2S_3 (1.0 mmol; Strem, 99.99%), CuO (2.0 mmol; Alfa, 99.99%), and KI (2.4 mmol, Aldrich, 99%) to aid in crystallization. The tube was sealed under 10^{-4} Torr atmosphere and then placed in a computer-controlled furnace. The sample was heated from 298 K to 1173 K in 15 h, held at 1173 K for 96 h, cooled to 573 K at 2 K/h, and then cooled to 298 K in 10 h. The reaction mixture was next washed with deionized water and dried with acetone. The yield of red needles was 60−70%. The compound is stable in air.

EDX Analysis of $La_5Cu_{6.33}O_4S_7$. Energy-Dispersive X-ray (EDX) analyses were carried out with the use of a Hitachi S-3400 SEM. Data were collected with an accelerating voltage of 20 keV, a working distance of 10 mm, and a collection time of 100 s. Selected single crystals of $La_5Cu_{6.33}O_4S_7$ showed the presence of La, Cu, O, and S, but not of K or I.

Structure Determination of $La_5Cu_{6.33}O_4S_7$. Single-crystal X-ray diffraction data were obtained on a single crystal of $La_5Cu_{6.33}O_4S_7$ at 153 K. Crystal data were collected on a Bruker Smart 1000 CCD diffractometer with the use of monochromatized MoKα radiation ($\lambda = 0.71073$ Å). The crystal-to-detector distance was 5.023 cm. The exposure time was 15 s/frame. Crystal decay was monitored by collecting 50 initial frames at the end of the data collection. The diffracted intensities were generated by a scan of 0.3° in ω in groups of 606 frames for each of the φ settings 0°, 90°, 180°, and 270°. Intensity data were collected with the program SMART.[16] Cell refinement and data reduction were carried out with the program SAINT,[16] and a numerical face-indexed absorption correction was made with the use of the program XPREP.[17] Finally, the program SADABS[17] was employed to make incident beam and decay corrections.

The structure was solved in the space group *Imma* of the orthorhombic system with the use of the direct-methods program SHELXS;[17] it was refined with the least-squares program SHELXL.[17] The refinement included anisotropic displacement parameters and a secondary extinction correction. Atom S5 is disordered over two positions separated by 0.584(8) Å. In contrast to the structure of $La_5Cu_6O_4S_7$, in the penultimate refinement considerable electron density was found between the layers. This density was subsequently assigned to a Cu3 atom whose occupancy converged to 0.32(7) in the final refinement. The only feature to note is that the ellipsoid associated with the Cu3 atom had principal mean-square displacements of 0.140, 0.034, and 0.028 Å^2. This suggests that there may be some disorder of the Cu3 atom. Attempts to model the disorder were not successful. Note that a similar refinement on data collected from a different crystal selected from a different reaction batch led to a structure that did not differ significantly; in particular, an occupancy of 0.34(7) was found for atom Cu3. The X-ray data do not allow an unequivocal assignment

(12) Chan, G. H.; Deng, B.; Bertoni, M.; Ireland, J. R.; Hersam, M. C.; Mason, T. O.; Van Duyne, R. P.; Ibers, J. A. *Inorg. Chem.* **2006**, *45*, 8264–8272.
(13) Ijjaali, I.; Mitchell, K.; Haynes, C. L.; McFarland, A. D.; Van Duyne, R. P.; Ibers, J. A. *J. Solid State Chem.* **2003**, *176*, 170–174.
(14) Hiramatsu, H.; Ueda, K.; Kamiya, T.; Ohta, H.; Hirano, M.; Hosono, H. *J. Phys. Chem. B* **2004**, *108*, 17344–17351.
(15) Huang, F. Q.; Brazis, P.; Kannewurf, C. R.; Ibers, J. A. *J. Solid State Chem.* **2000**, *155*, 366–371.
(16) Bruker. *SMART Version 5.054 Data Collection and SAINT-Plus Version 6.45a Data Processing Software for the SMART System*; Bruker Analytical X-Ray Instruments, Inc.: Madison, WI, 2003.
(17) Sheldrick, G. M. *Acta Crystallogr., Sect. A: Found. Crystallogr.* **2008**, *64*, 112–122.

Table 1. Crystal Data and Structure Refinement for $La_5Cu_{6.33}O_4S_7$

	$La_5Cu_{6.33}O_4S_7$
formula mass	1385.18
space group	*Imma*
Z	4
a, Å	5.6746(6)
b, Å	15.6402(15)
c, Å	17.5345(17)
V, Å^3	1556.2(3)
T, K	153(2)
λ, Å	0.71073
ρ_c, g cm^{-3}	5.912
μ, cm^{-1}	227.84
$R(F)^a$	0.038
$R_w(F^2)^b$	0.092

^{a} $R(F) = \sum||F_o|-|F_c||/\sum|F_o|$ for $F_o^2 > 2\sigma(F_o^2)$. ^{b} $R_w(F_o^2) = [\sum w(F_o^2 - F_c^2)^2/\sum wF_o^4]^{1/2}$, $w^{-1} = \sigma^2(F_o^2) + (0.05 \times F_o^2)^2$ for $F_o^2 > 0$; $w^{-1} = \sigma^2(F_o^2)$ for $F_o^2 \leq 0$.

of Cu as the interstitial atom. However, ICP analysis (see below) confirms the stoichiometry that results if the assignment is to Cu. From these results it is clear that this compound is nonstoichiometric with formula $La_5Cu_{6.33}O_4S_7$. Additional experimental details are shown in Table 1 and in the Supporting Information.

Inductively Coupled Plasma (ICP) Measurement. A VISTA-MPX CCD Simultaneous Varian ICP-OES was used to measure the molar ratio of Cu/La for $La_5Cu_{6.33}O_4S_7$. Single crystals (1.1 mg) of $La_5Cu_{6.33}O_4S_7$ were dissolved in 0.45 mL of HNO_3, and the solution was adjusted to a volume of 15 mL with MQ water. The Cu/La molar ratio was determined to be 1.25(2):1. The ratio expected from the composition $La_5Cu_{6.33}O_4S_7$ is 1.27:1. Note, the composition determined from ICP came from a sampling of a number of crystals, and it is possible that the compositions of the crystals used for physical properties measurements may be slightly different.

Magnetic Susceptibility of $La_5Cu_{6.33}O_4S_7$. Direct current magnetic susceptibility measurements on single crystals of $La_5Cu_{6.33}O_4S_7$ were carried out with the use of a Quantum Design MPMS5 SQUID magnetometer. The sample comprised 52.3 mg of single crystals of $La_5Cu_{6.33}O_4S_7$ that were ground and loaded into a gelatin capsule. In the temperature range between 1.8 and 380 K susceptibility measurements were collected with a 500 G applied field. The susceptibility data were corrected for core diamagnetism.[18]

Single crystal Absorption Measurement of $La_5Cu_{6.33}O_4S_7$. Polarized (0° and 90°) and unpolarized absorption measurements of the (010) crystal face were performed on a single crystal of $La_5Cu_{6.33}O_4S_7$ with the use of equipment and techniques described earlier.[19,20] The optical band gap was calculated by means of a linear regression technique.[21,22]

Electrical Conductivity of $La_5Cu_{6.33}O_4S_7$. The compositions of two red needles of $La_5Cu_{6.33}O_4S_7$ were confirmed with EDX measurements. The electrical conductivity (146 to 340 K) of each of these two single crystals was obtained with the use of a computer-controlled four-probe technique.[23] Electrical contacts consisted of fine gold wires attached to the crystals with gold paste. To improve the contact performance, the samples were placed under vacuum for at least 24 h to allow the gold paste to cure completely. Excitation currents were kept as low as possible, typically below 1 mA, to minimize any nonohmic voltage responses at the contact-sample interface, and they were rapidly switched to minimize any thermoelectric effects. For each crystal, measurements of the sample cross-sectional area and voltage probe separation were made with a calibrated eyepiece on a binocular microscope.

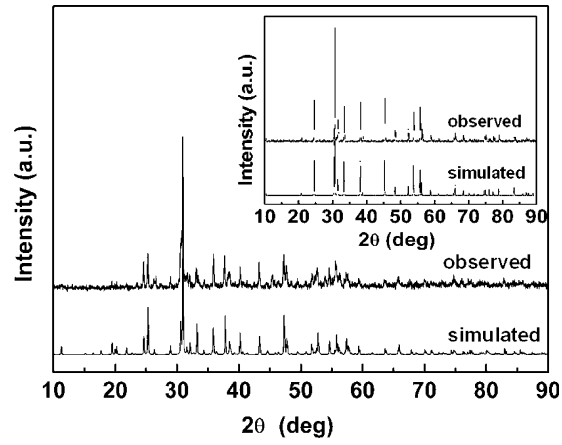

Figure 1. X-ray diffraction patterns of $La_5Cu_6O_4S_7$ and LaCuOS (inset) powders compared to those calculated from the known crystal structures.

Results and Discussion

Syntheses. The synthesis of single crystals of $La_5Cu_{6.33}O_4S_7$ produced two major products, red needles (~60−70%) and orange polycrystalline material (~20%). The KI flux proved to be crucial in promoting crystallization and in improving the overall yield of the reaction. Attempts (for example, slow cooling and the use of various potassium halide fluxes) were made to grow larger crystals for Hall measurements, but these were unsuccessful.

Earlier, orange single crystals of $La_5Cu_6O_4S_7$ were synthesized in about 50−60% yield by the solid-state reaction of stoichiometric amounts of La_2S_3 (1.0 mmol; Strem, 97%), CuO (2.0 mmol; Alfa, 99.99%), and KI (2.4 mmol, Aldrich, 99.99+%) to aid in crystallization.[15] The present attempts to repeat this procedure did not afford any orange crystals of $La_5Cu_6O_4S_7$ but rather red crystals of $La_5Cu_{6.33}O_4S_7$ in about 60−70% yield. Despite numerous variations of the procedure, no single crystals of $La_5Cu_6O_4S_7$ were obtained.

However, a powder of $La_5Cu_6O_4S_7$ was obtained by the stoichiometric reaction of La_2O_3, Cu, La_2S_3, and S. With these same reactants in stoichiometric proportions, a powder sample of LaCuOS was also synthesized. An X-ray diffraction powder pattern of $La_5Cu_6O_4S_7$ collected at 298 K is compared to the pattern calculated from the known crystal structure determined at 153 K (Figure 1).[15] In the inset to Figure 1a similar comparison is made for LaCuOS collected here with that calculated from the known crystal structure,[9] both determined at 298 K. The two materials appear to be pure within the limitations of the method.

(18) *Theory and Applications of Molecular Diamagnetism*; Mulay, L. N., Boudreaux, E. A., Eds.; Wiley-Interscience: New York, 1976.
(19) Mitchell, K.; Huang, F. Q.; Caspi, E. N.; McFarland, A. D.; Haynes, C. L.; Somers, R. C.; Jorgensen, J. D.; Van Duyne, R. P.; Ibers, J. A. *Inorg. Chem.* **2004**, *43*, 1082–1089.
(20) Chan, G. H.; Sherry, L. J.; Van Duyne, R. P.; Ibers, J. A. *Z. Anorg. Allg. Chem.* **2007**, *633*, 1343–1348.
(21) Pankove, J. I. *Optical Processes in Semiconductors*; Prentice-Hall, Inc: Englewood Cliffs, NJ, 1971.
(22) Deng, B.; Chan, G. H.; Ellis, D. E.; Van Duyne, R. P.; Ibers, J. A. *J. Solid State Chem.* **2005**, *178*, 3169–3175.
(23) Lyding, J. W.; Marcy, H. O.; Marks, T. J.; Kannewurf, C. R. *IEEE Trans. Instrum. Meas.* **1988**, *37*, 76–80.

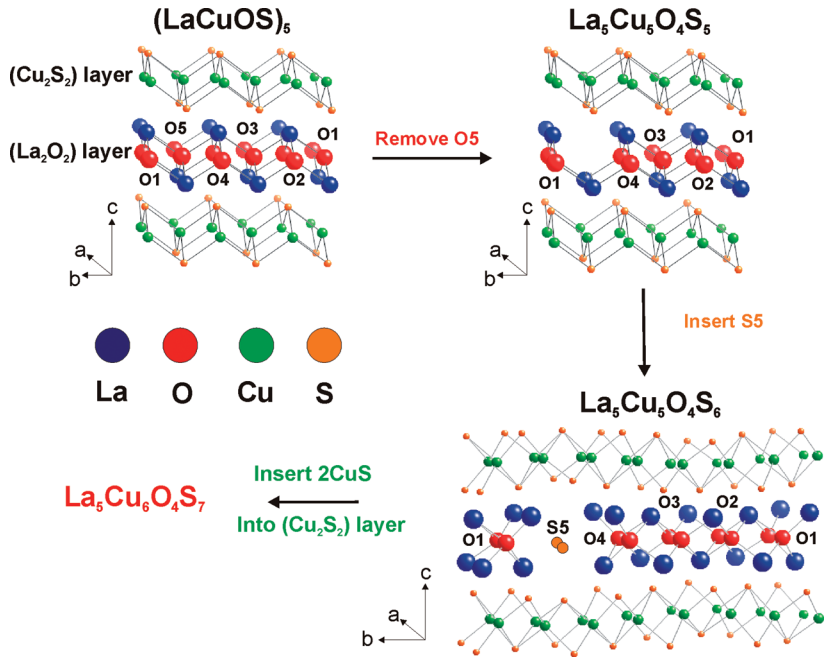

Figure 2. Illustration of the relationship between LaCuOS and $La_5Cu_6O_4S_7$. La−S bonds have been removed for clarity.

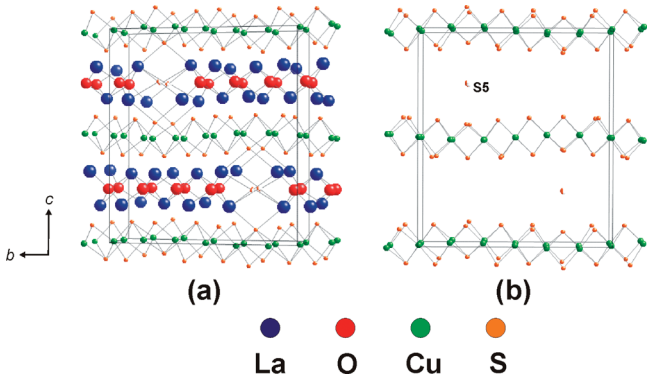

Figure 3. View nearly down [100] of (a) the unit cell of $La_5Cu_6O_4S_7$ and (b) the same cell with La, and O atoms removed to show only $^2_\infty[Cu_6S_6^{5-}]$ layers and atom S5.

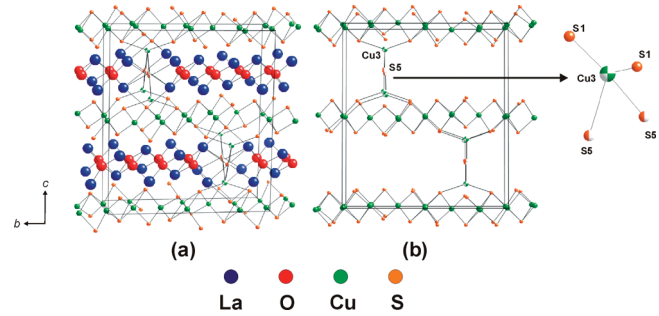

Figure 4. View nearly down [100] of (a) the unit cell of $La_5Cu_{6.33}O_4S_7$ and (b) the same cell with La, and O atoms removed to show only $^2_\infty[Cu_6S_6^{5-}]$ layers and atom S5. The coordination environment of the Cu3 atom is shown on the right.

Crystal Structures. Details of the crystal structures of stoichiometric $La_5Cu_6O_4S_7$ and LaCuOS have been described previously.[9,15] The structure of LaCuOS is shown in Figure 2 and that of $La_5Cu_6O_4S_7$ is shown in Figure 3. Conceptually (Figure 2), if every fifth O atom in the $^2_\infty[La_2O_2^{2+}]$ layer in the LaCuOS structure is replaced with an S atom (S5) in an ordered way and CuS is inserted into the $^2_\infty[Cu_2S_2^{2-}]$ layer then the structure of $La_5Cu_6O_4S_7$ results. One starts with alternating $^2_\infty[La_2O_2^{2+}]$ and $^2_\infty[Cu_2S_2^{2-}]$ layers in the LaCuOS structure and ends up with alternating $^2_\infty[La_5O_4S^{5+}]$ and $^2_\infty[Cu_6S_6^{5-}]$ layers in $La_5Cu_6O_4S_7$. From charge balance, the average oxidation state of Cu is 7/6+ in the $^2_\infty[Cu_6S_6^{5-}]$ layer, with one Cu^{2+} center for each of five Cu^{1+} centers. These are not distinguishable crystallographically; the unit cell contains only two crystallographically independent Cu centers. Because an S atom is larger than an O atom, the incorporation of S atoms into the $^2_\infty[La_2O_2^{2+}]$ layer expands it. The space group changes from *P*4/*nmm* in LaCuOS to *Imma* in $La_5Cu_6O_4S_7$. The introduction of Cu^{2+} into the $^2_\infty[Cu_2S_2^{2-}]$ layer and S atoms into the $^2_\infty[La_2O_2^{2+}]$ layer results in optical and transport properties of $La_5Cu_6O_4S_7$ that are different from those of LaCuOS.

The unit cell of nonstoichiometric $La_5Cu_{6.33}O_4S_7$ is shown in Figure 4. The coordination environments of the La and Cu1 and Cu2 atoms of both the stoichiometric and nonstoichiometric compounds are similar. Each La1 and La3 atom is coordinated to four O and four S atoms to form a distorted square antiprism. Atom La2 is coordinated to six S atoms and two O atoms. Each Cu1 and Cu2 atom is coordinated to four S atoms to form a distorted tetrahedron. However, the two structures differ in an important way. In $La_5Cu_{6.33}O_4S_7$, there are now three crystallographically independent Cu centers in the unit cell. In Figures 3b and 4b, the La and O atoms have been removed to enable one to visualize how the additional Cu3 atom connects the $^2_\infty[La_5O_4S^{5+}]$ and $^2_\infty[Cu_6S_6^{5-}]$ layers through a distorted tetrahedral coordination of four S atoms, two from each layer.

In $La_5Cu_{6.33}O_4S_7$, the incorporation of ~ 0.33 Cu atoms leads to an average Cu oxidation state of ~1.11 in contrast to that of 1.17 in $La_5Cu_6O_4S_7$. The introduction of Cu^{1+} atoms between the $^2_\infty[La_5O_4S^{5+}]$ and $^2_\infty[Cu_6S_6^{5-}]$ layers of

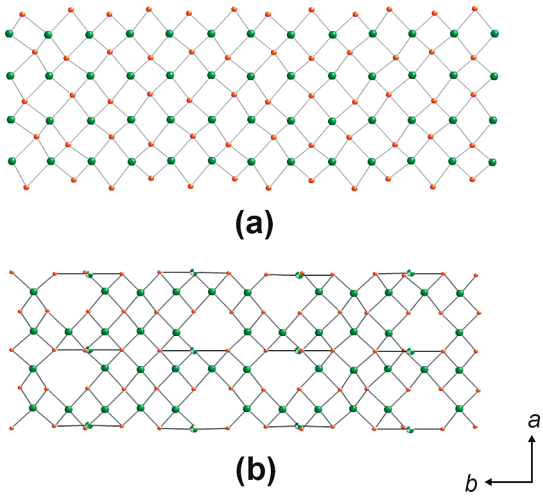

Figure 5. Projection down [001] of the $^2_\infty[Cu_6S_6^{5-}]$ layer in (a) $La_5Cu_6O_4S_7$ and (b) $La_5Cu_{6.33}O_4S_7$.

Table 2. Selected Interatomic Distances (Å) for $La_5Cu_{6.33}O_4S_7$

La1−O1 × 2	2.444(3)	Cu1−S2	2.506(2)
La1−O2 × 2	2.343(3)	Cu1−S3	2.339(2)
La1−S1	3.044(2)	Cu1−S4	2.406(2)
La1−S2 × 2	3.238(1)	Cu2−S1 × 2	2.441(2)
La1−S4	3.185(1)	Cu2−S2 × 2	2.417(2)
La2−O1 × 2	2.341(3)	Cu3−S1 × 2	2.624(3)
La2−S1 × 2	3.239(1)	Cu3−S5[a] × 2	2.326(9)
La2−S2	3.114(2)	Cu1−Cu1	2.643(1)
La2−S3	2.964(2)	Cu1−Cu1	2.662(1)
La2−S5[a] × 2	2.966(6)	Cu1−Cu1	3.012(1)
La3−O2 × 4	2.385(3)	Cu1−Cu2 × 2	2.5967(6)
La3−S2 × 2	3.180(2)	Cu2−Cu2 × 2	2.808(2)
La3−S4 × 2	3.180(1)	Cu2−Cu2	2.866(2)
Cu1−S1	2.375(2)		

[a] Closest S5 of the disordered pair.

$La_5Cu_6O_4S_7$ alters the crystal structure of the resultant $La_5Cu_{6.33}O_4S_7$ compound and disrupts the connectivity of the $^2_\infty[Cu_6S_6^{5-}]$ layer (Figure 5). The result is a dramatic difference between the transport properties of nonstoichiometric $La_5Cu_{6.33}O_4S_7$ and those of stoichiometric $La_5Cu_6O_4S_7$.

Table 2 summarizes some interatomic distances in $La_5Cu_{6.33}O_4S_7$. Because of the disorder of the S5 atom and the possible disorder of the Cu3 atom the metrical details of the Cu3 environment are not necessarily representative. Other distances are normal and in agreement with the ranges of comparable distances in LaCuOS[9] and $La_3CuO_2S_3$.[24]

Magnetic Susceptibility of $La_5Cu_{6.33}O_4S_7$. The molar magnetic susceptibility χ_m of crushed single crystals of $La_5Cu_{6.33}O_4S_7$ as a function of temperature is shown in the Supporting Information. Between 1.8 and 2.7 K the susceptibility is positive and is consistent with the small concentration of Cu^{2+} ($3d^9$), as expected from charge balance. Above 2.7 K, the susceptibility is negative and diamagnetic.

Optical Properties. The optical absorption spectra at 298 K of pulverized powders of $La_5Cu_6O_4S_7$ and LaCuOS are depicted in Figure 6. A sharp drop in absorption at about 619 nm corresponds to the fundamental absorption edge. The band gap (E_g = 2.0 eV), estimated by a straightforward extrapolation method without taking into account the exciton absorption, is smaller than that of LaCuOS (E_g = 3.1 eV). The introduction of S atoms into the $^2_\infty[La_2O_2^{2+}]$ layer of LaCuOS to form the $^2_\infty[La_5O_4S^{5+}]$ layer in $La_5Cu_6O_4S_7$ and the incorporation of d^9 electrons of Cu^{2+} ions result in a decrease of the optical band gap. Not surprisingly, this decrease results in an increase in the electrical conductivity (Table 3).

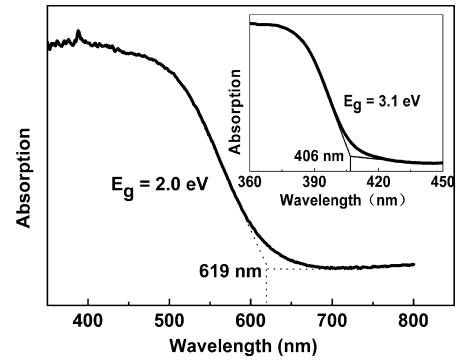

Figure 6. Absorption spectra of bulk $La_5Cu_6O_4S_7$ and LaCuOS (inset).

Figure 7a depicts the single-crystal optical absorption spectrum obtained with unpolarized light perpendicular to the (010) crystal face of $La_5Cu_{6.33}O_4S_7$. The single crystal was mounted along the [100] direction. The band gap (E_g = 2.0 eV) is assumed to be a direct transition. The incorporation of a small concentration Cu^{1+} ($3d^{10}$) between the $^2_\infty[La_5O_4S^{5+}]$ and $^2_\infty[Cu_6S_6^{5-}]$ layers of $La_5Cu_6O_4S_7$ does not significantly alter the optical properties. Note that the absorption spectrum of the (001) crystal face of the same $La_5Cu_{6.33}O_4S_7$ single crystal showed no visible absorption edge; the crystal appeared to be black in that direction. The absorption spectrum obtained with polarized light of the (010) face of $La_5Cu_{6.33}O_4S_7$ is shown in Figure 7b,c. The dichroism is consistent with the orthorhombic symmetry of the compound.

Transport Properties. The electrical conductivity of a sintered disk of stoichiometric $La_5Cu_6O_4S_7$ as a function of temperature is shown in Figure 8. The electrical conductivity is $\sim 10^2$ to 10^3 times larger than that of LaCuOS (inset of Figure 8) with $\sigma_{electrical}$ being 2.18 S cm^{-1} at 298 K. The Hall coefficient is +9 cm^3 C^{-1}, and the mobility (μ) is + 20.1 cm^2 V^{-1} s^{-1} at 298 K. The Seebeck coefficient is positive from 250 to 500 K (Figure 9), which indicates that $La_5Cu_6O_4S_7$ is a *p*-type conductor. The electrical conductivity along [100] of a single crystal of $La_5Cu_6O_4S_7$ was previously reported to be 2.6 10^4 S cm^{-1} at 298 K.[15] That the conductivity of a single crystal of $La_5Cu_6O_4S_7$[15] is so much greater than that of the sintered disk is not surprising. $La_5Cu_6O_4S_7$ is not only anisotropic in its optical properties but also in its transport properties. From the crystal structure and band structure calculations,[15] the conductivity perpendicular to the layers (along [001]) should be much smaller than that along the layers. The conductivity of the single crystal was determined along the layers, specifically in the [100] direction. The measurement on the sintered disk is an average over all orientations. Moreover, grain boundaries and defects in the sintered disk impede the transport of charge carriers. Both the single crystal and the sintered disk exhibited metallic behavior.

(24) Ijjaali, I.; Haynes, C. L.; McFarland, A. D.; Van Duyne, R. P.; Ibers, J. A. *J. Solid State Chem.* **2003**, *172*, 257–260.

Table 3. Transport and Optical Properties of LnCuOS (Ln = La−Nd), $La_5Cu_6O_4S_7$, and $La_5Cu_{6.33}O_4S_7$ at 298 K[a]

compound	σ (S cm^{-1})	Seebeck (μV K^{-1})	μ (cm^2 V^{-1} s^{-1})	E_g (eV)	reference
LaCuOS	8.0×10^{-6}	+150		3.14	10
LaCuOS				3.1	this work
$La_{0.95}Sr_{0.05}CuOS$	0.19	+3			10
CeCuOS	0.61	+12			10
$CeCu_{0.8}OS$	9.8×10^{-3}		1.5	<0.73	12
PrCuOS	1.6×10^{-5}	+340		3.03	10
$Pr_{0.95}Sr_{0.05}CuOS$	1.8	+9			10
NdCuOS	3.8×10^{-4}	+97		2.98	10
$La_5Cu_6O_4S_7$[b]	2.6×10^4				15
$La_5Cu_{6.33}O_4S_7$[b]	4.5×10^{-3}			2.0; (010)	this work
$La_5Cu_6O_4S_7$	2.18	+20	20.1	2.0	this work

[a] Transport measurements conducted on a sintered disk unless otherwise noted. [b] Measured along [100] of a single crystal.

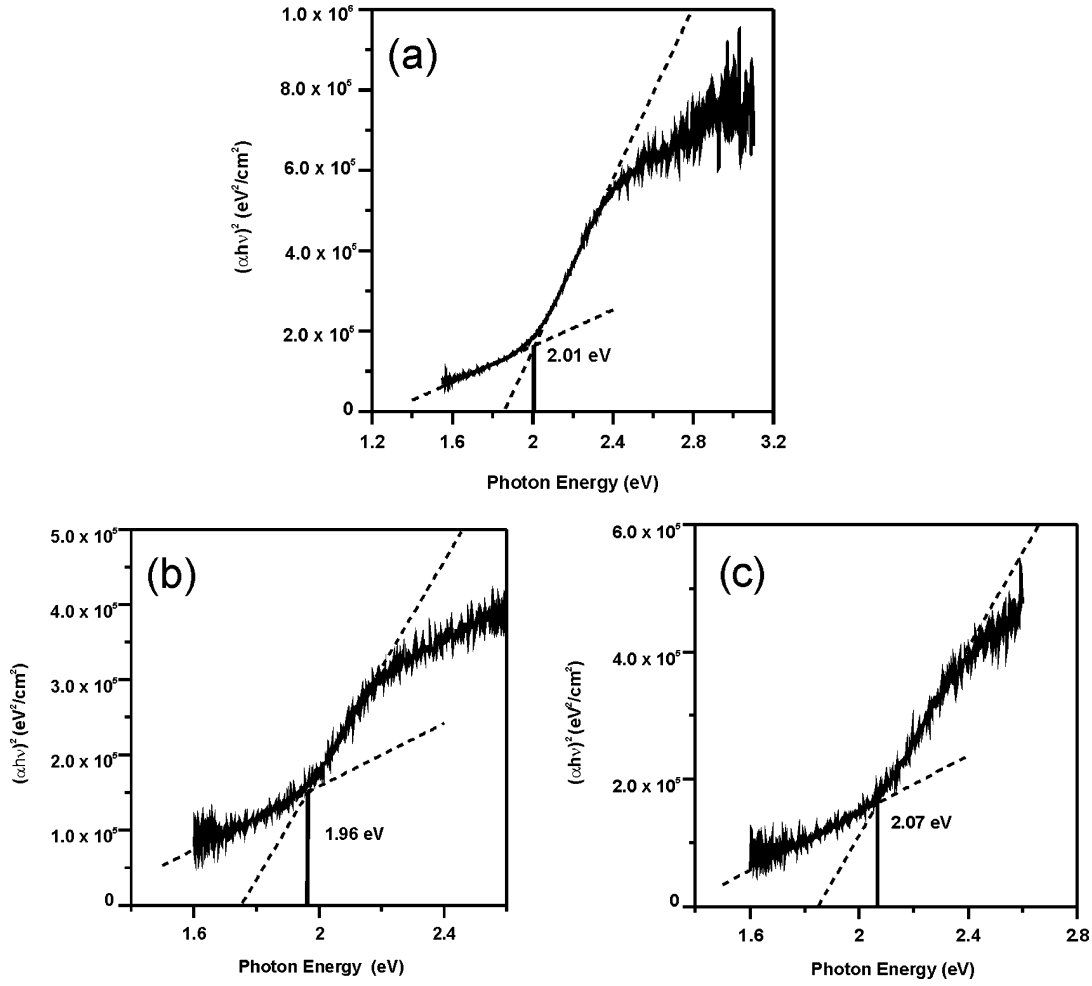

Figure 7. Optical spectrum of a single crystal of $La_5Cu_{6.33}O_4S_7$ with light perpendicular to the (010) crystal face (a) unpolarized, (b) 90°, and (c) 0°.

The increase in electrical conductivity of $La_5Cu_6O_4S_7$ relative to LaCuOS and related materials is the result of different internal structures and is not the result of doping or vacancies (Table 3). In LaCuOS, the oxidation state of Cu is 1+, whereas in $La_5Cu_6O_4S_7$, the average oxidation state is 7/6+. Consequently, there is an increase in potential hole carriers in $La_5Cu_6O_4S_7$ compared to LaCuOS. Moreover, the bulk material exhibits metallic-like conductivity. In a band-structure calculation[15] this metallic conductivity was attributed to a drop in the Fermi level where Cu−Cu antibonding 3d states become unoccupied and Cu−Cu interactions increase leading to a metallic $^2_\infty[Cu_6S_6^{5-}]$ layer.

The electrical conductivity along [100] of a single crystal of nonstoichiometric $La_5Cu_{6.33}O_4S_7$ as a function of temperature is shown in Figure 10. The value of $\sigma_{electrical}$ is 4.5(1) $\times$ 10^{-3} S/cm at 298 K. The conductivity rises rapidly between about 150 and 225 K and then increases more slowly as the temperature increases. As opposed to the metallic behavior of stoichiometric $La_5Cu_6O_4S_7$, nonstoichiometric $La_5Cu_{6.33}O_4S_7$ is a semiconductor. This difference can be attributed to the crystal structure. The disruption of the $^2_\infty[Cu_6S_6^{5-}]$ and the decrease in the overall Cu^{2+} ($3d^9$) concentration lead to a significant decrease in the electrical conductivity, and the randomly and partially occupied Cu3 sites may reduce the charge-carrier mobility.

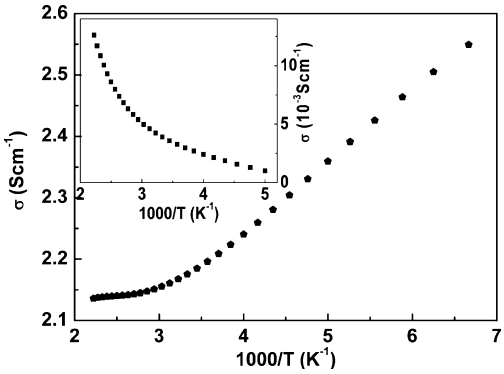

Figure 8. Electrical conductivity σ as a function of T^{-1} of sintered disks of $La_5Cu_6O_4S_7$ and LaCuOS (inset).

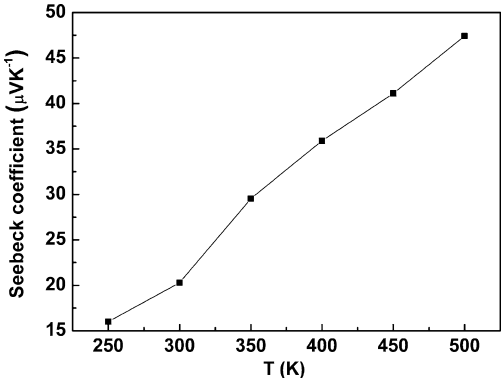

Figure 9. Temperature dependence of the Seebeck coefficient of a $La_5Cu_6O_4S_7$ sintered disk.

Acknowledgment. This research was supported in part by the National Science Foundation Grant DMR00-96676 and in part by the U.S. Department of Energy Grant BES ER-15522 (J.A.I.). Use was made of the Central Facilities supported by the MRSEC program of the National Science Foundation (DMR05-20513) at the Materials Research Center of Northwestern University. We thank Dr. Kenneth G. Spears for the use of his NIR spectrometer. F.Q.H. gratefully acknowledges support from the National 973 Program of China Grant 2007CB936704.

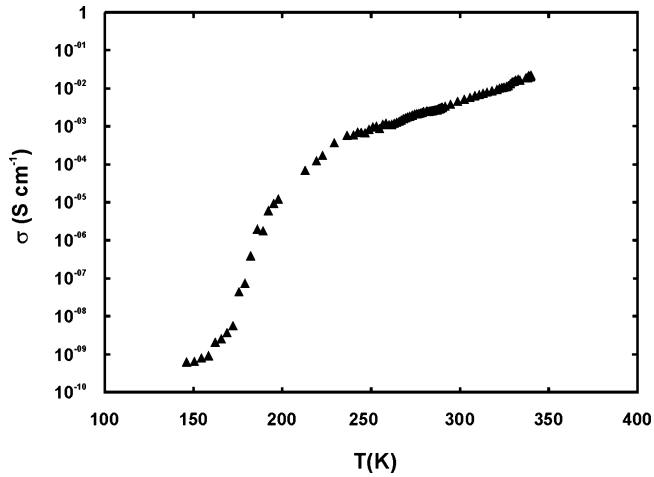

Figure 10. Electrical conductivity (log scale) along [100] vs T of a single crystal of $La_5Cu_{6.33}O_4S_7$.

Supporting Information Available: A crystallographic file in CIF format and the molar susceptibility χ_m versus temperature T for $La_5Cu_{6.33}O_4S_7$. This material is available free of charge via the Internet at http://pubs.acs.org.

IC7024796